

# Results from the commissioning of the ATLAS Pixel detector

Jedrzej Biesiada<sup>\*,a</sup>, on behalf of the ATLAS collaboration

<sup>a</sup>Lawrence Berkeley National Laboratory, Physics Division, MS50B-6222, 1 Cyclotron Road, Berkeley, CA 94720, USA

---

## Abstract

The ATLAS Pixel detector is a high-resolution, low-noise silicon-based device designed to provide tracking and vertexing information within a distance of 12 cm from the LHC beam axis. It consists of approximately 80 million pixel channels with radiation-hard front-end electronics connected through optical fibers to a custom-controlled DAQ system away from the detector. Following the successful installation of the detector in June 2007, an intense commissioning period was conducted in the year 2008 and more than 400,000 cosmic-ray tracks were recorded in conjunction with other ATLAS sub-detectors. By the end of the year, 96% of the detector was tuned, calibrated, and taking data at 99.8% tracking hit efficiency and with noise occupancy at the  $10^{-10}$  level. We present here the results of the commissioning, calibration, and data-taking as well as the outlook for future performance with LHC collision-based data.

*Key words:*

Silicon pixel detector, ATLAS detector commissioning

---

## 1. Introduction

The ATLAS detector [1] is one of two general-purpose detectors that will study fundamental high-energy physics in proton-proton collisions produced by the Large Hadron Collider (LHC). The Inner Detector tracker is the sub-detector closest to the beam-pipe; it consists of three components: the Transition Radiation Tracker (TRT), the Silicon Central Tracker (SCT), and the Pixel detector. The Pixel detector [2] is the inner-most of the three components and the most granular, as it is designed to provide the lowest-occupancy measurements that are critical for efficient and accurate pattern recognition and for vertex reconstruction (including both the primary collision vertex and secondary vertices formed by decays of long-lived particles). The detector uses silicon pixel technology designed to withstand the high-radiation environment of the inner regions of the tracker.<sup>1</sup>

## 2. Overview of the Pixel detector

### 2.1. Geometrical layout

The Pixel detector consists of a central barrel region of three cylindrical layers at radii of 50.5, 88.5, and 122.5 mm from the beam axis; and two end-caps, one on each side of the barrel, consisting of three disks located at 495, 580, and 650 mm away from the nominal interaction point along the

beam axis. The barrel and end-caps provide three space-point tracking in the pseudorapidity region  $\eta < 2.5$ . The detector is composed of 1744 modules, each of which contains 46,080 pixel channels divided among 16 front-end chips (FE), for a total of approximately 80 million channels.

### 2.2. Pixel modules

Pixel modules consist of  $n^+$  pixel sensors implanted on  $n$ -doped bulk wafers with a  $p^+$  backplane, designed and qualified to withstand an integrated radiation dose of 50 MRad. Bulk depth is 250  $\mu\text{m}$ , while most pixel dimensions are 50  $\mu\text{m} \times 400 \mu\text{m}$ .<sup>2</sup> The FE chips are bump-bonded to the pixels and utilize 0.25  $\mu\text{m}$  CMOS technology to perform pre-amplification, discrimination, measurement of time over threshold (TOT), and digitization of the sensor signals. A high-density-interconnection Kapton/Copper printed circuit (flex board) is connected to the FE chips with wire bonds and contains a module control chip (MCC) that communicates with the chips and multiplexes FE data, as well as performing basic error detection in the data stream. The flex board also contains connections to the optical readout system and the power and HV distribution, as well as an NTC thermistor for temperature measurement.

### 2.3. Readout

On-detector optoboards convert the electrical MCC signals from six to seven modules into optical form with VCSEL lasers and transmit them through optical fibers to

---

\*Corresponding author. Tel.: +41-76-487-4549; fax: +1-510-486-5101.

Email address: [jbiesiada@lbl.gov](mailto:jbiesiada@lbl.gov) (Jedrzej Biesiada)

<sup>1</sup>The fluence of charged particles at a radius of 5 cm is expected to be  $3 \times 10^7 \text{ cm}^{-2} \text{ sec}^{-1}$ .

<sup>2</sup>Some pixels are larger to bridge the regions between FE chips.

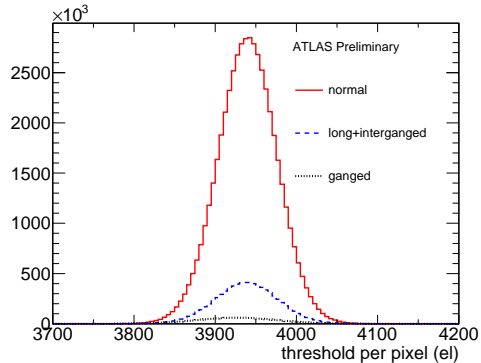


Figure 1: Tuned threshold distribution for the whole detector.

the off-detector electronics. The optoboards are operated at about 20°C to provide low bit-error-rate data transmission in the VCSELs. Off-detector DAQ boards convert the signal back to electrical form, format and monitor the data stream, and pass it on to the global ATLAS DAQ stage. The same path is engaged in reverse for module configuration and control data, with VCSELs on the DAQ boards transmitting multiplexed clock and command information through separate optical fibers.

### 3. Installation and calibration

#### 3.1. Installation

The Pixel package was inserted into the center of the Inner Detector in June of 2007. However, cable connection could not commence until February of 2008 due to other ATLAS installation constraints and was finished by April 2008.

The cooling system [3] was commissioned loop by loop until all 88 loops servicing the detector were operating at the end of August 2008. Three loops were found to have significant leaks inside of the detector package and will be monitored as a potential source of inefficiency in the future. (They cannot be fixed and the  $C_3F_8$  coolant leaks will be studied to see if they could cause structural defects or corrosive damage due to HF recombination in a radiation environment after LHC turn-on.) The evaporative temperature in 2008 was  $-10^\circ\text{C}$ , leading to module temperatures of roughly  $-5^\circ\text{C}$ .

#### 3.2. Calibration

The exposure of the Pixel detector to high radiation doses during operation leads to modest changes in performance of the electronics and sensors. To retain the initial performance throughout the detector lifetime, it is essential to regularly tune and calibrate the modules in the detector. During 2008, we have performed a first set of reference calibrations that will serve as our performance baseline. The calibration consisted of tuning of the optical readout; measurement and tuning of the signal threshold for pixel uniformity; tuning of the TOT to set the charge

response for a minimum-ionizing particle (MIP); and TOT calibration to characterize the charge response over the whole dynamic range of the pixels.

##### 3.2.1. Optical tuning

The optical error rate is measured versus the threshold and phase of the off-detector optical PIN receiver and versus the on-detector VCSEL laser power. Two methods are used: a faster one, where the modules are asked to send back 20 MHz clock and the 'one' bits are counted; and a slower one, where the modules send back a pseudo-random bit pattern and a bit-by-bit comparison is performed. The more accurate slower method would only be used on problematic modules.

##### 3.2.2. Threshold calibration

The pixel FE electronics have the capacity to inject charge directly into the pixel preamplifier. While injecting many signals, the number of hits that are read out is counted versus the size of the injected charge, which is scanned through the expected threshold. The resulting turn-on curve convoluted with roughly Gaussian noise in the pixel is fitted to an Error function, with the fitted mean corresponding to the threshold and the fitted width corresponding to the noise. The threshold is tuned pixel by pixel to the value of 4000 electrons, reducing the threshold dispersion from 100 to 40 electrons (Fig. 1). The threshold-over-noise ratio for most pixels is around 25, resulting in low probability of noise hits.

##### 3.2.3. TOT tuning and calibration

The TOT pulse width is proportional to the signal charge through a constant-current feedback in the pixel preamplifier and is measured in units of bunch crossings (BC), equivalent to 25 ns at the 40 MHz LHC clock. The TOT value can be tuned at the FE level and fine-tuned at the pixel level. The pixel charge response is almost linear over a large range of deposited charge. This behavior introduces a trade-off between signal size and the dynamic range, since if the TOT is longer than the ATLAS Level-1 trigger latency, the hit is lost. The current tuning is set to a TOT of 30 BC for a MIP charge deposition (roughly 20,000 electrons), giving a dynamic range of 8 MIPs. The tuning has reduced the TOT dispersion over the whole detector by 50%.

##### 3.2.4. DAQ firmware upgrade and HV leakage current

The calibration is controlled by digital signal processors in the DAQ boards, which run firmware binaries that are maintained and developed within the Pixel group. In 2008, a new version of the firmware was introduced, incorporating a more versatile modular design and various functional optimizations. As a result, most calibration functions perform two to four times faster, and new tasks have been implemented to exploit the full calibration functionality of the FE chips. One of these tasks is the leakage scan,

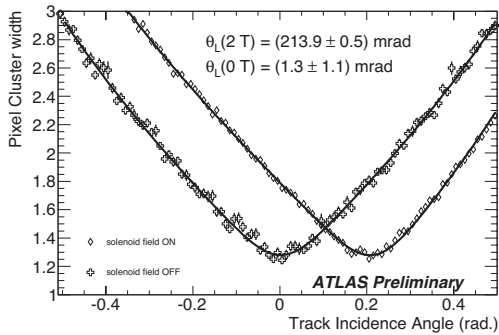


Figure 2: Distribution of the cluster width versus track incidence angle for the Pixel detector for two values of the magnetic field, showing the fitted Lorentz-angle values.

which measures the HV leakage current pixel by pixel. The pre-irradiation baseline shows that approximately 99% of pixels in the detector do not presently draw measurable current. We expect roughly 25 nA per pixel at the end of lifetime at  $-5^{\circ}\text{C}$ .

#### 4. Taking data with cosmic rays

When single beams were first injected into the LHC on Sept. 10, 2008, the Pixel detector did not collect data as it was operated with HV turned off and the FE preamplifiers disabled to protect the FE chips from large charge depositions that are possible in unstable beam conditions. After the LHC incident of September 19, more than 400,000 tracks with hits in the Pixel detector were collected over several months of data-taking with cosmic rays, interleaved with the calibration efforts. After masking roughly 0.01% of noisy pixels in the detector, noise occupancy at the  $10^{-10}$ -per-BC level was achieved, corresponding to roughly 0.05 noise hits per event in the whole detector.

##### 4.1. Timing

The Pixel detector was reading out a window of 8 consecutive BCs in order to allow synchronization with the other ATLAS sub-detectors, which was quickly achieved. As the detector is currently timed-in to within 3 BCs, the read-out window will be reduced to 5 BCs for initial LHC data, and ultimately to 1-3 BCs.

##### 4.2. Calibration studies with cosmic rays

The cosmic-ray data has been extensively analyzed for additional calibration measurements. Fig. 2 shows the cluster width in the pixel detector versus incidence angle of the track for two different values of the solenoidal magnetic field in the Inner Detector. The minimum of the distributions occurs at the Lorentz angle, which reflects the deflection of the charge carriers in the magnetic field. This angle is consistent with zero when the magnetic field is off and about 214 mrad for the full magnetic strength of

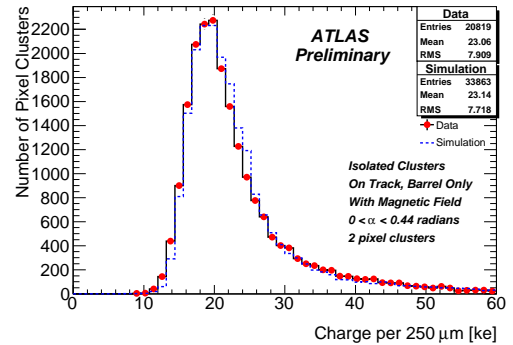


Figure 3: Distribution of the cluster charge distribution in data (points and fitted solid line) and simulation (dashed) for tracks with nearly normal incidence.

2 T. This result is consistent with simulated expectations to within 5%. Fig. 3 shows that the cluster-charge distribution for tracks with nearly normal incidence agrees very well with simulated events as well. Remaining disagreements are being studied to improve modeling of the detector response.

Misalignment of the Pixel detector has been reduced to the 20  $\mu\text{m}$  level in the 50  $\mu\text{m}$  pixel direction (azimuthal) and to 30  $\mu\text{m}$  in the 400  $\mu\text{m}$  direction (longitudinal) after extensive alignment efforts down to the module level in the central barrel. End-cap alignment will require LHC beam data. With the most recent aligned geometry, the efficiency of attaching a hit to a track traversing the barrel is 99.8%, which is compatible with the test-beam value of 99.9% [4].

#### 5. Conclusion and outlook

After an intensive commissioning and cosmic-ray data-taking period over the year 2008, 96% of the ATLAS Pixel detector is tuned, calibrated, and ready to collect data, with all but about 2% expected to be recovered. The cosmic-ray data sample has been used for extensive calibration, tuning of simulation input, and on-going studies of detector performance. After upgrade work on the cooling system concludes in May 2009, the detector will be re-calibrated in preparation for LHC collisions to be delivered by the end of 2009.

#### References

- [1] The ATLAS Collaboration, G. Aad et al., The ATLAS Experiment at the CERN Large Hadron Collider, JINST 3 (2008) S08003.
- [2] G Aad et al., ATLAS pixel detector electronics and sensors, JINST 3 (2008) P07007.
- [3] D. Attree et al., The evaporative cooling system for the ATLAS inner detector, JINST 3 (2008) P07003.
- [4] A. Andreazza, on behalf of the ATLAS Pixel Collaboration, Nucl. Instr. Meth. A 565 (2006) 23-29.